PROCEEDINGS - 36th ANNUAL CONDENSED MATTER AND MATERIALS MEETING, 31 Jan. -3 Feb. 2012. Wagga Wagga, NSW, Australia

Fabrication, Characterization and Applications of $Si_{1-x}Ti_xO_2$ (x= 0-1) Inverse Opal Photonic Crystals

Z.H. Al-Azri and G.I.N. Waterhouse

School of Chemical Sciences, University of Auckland, Auckland, New Zealand.
MacDiarmid Institute for Advanced Materials and Nanotechnology, New Zealand.

Photonic crystals (PCs) are expected to find widespread application in next generation optoelectronic devices due to their inherent optical properties which can be used to manipulate or inhibit the propagation of light. This study focuses on the fabrication of 3-dimensionally ordered macroporous (3DOM) inverse opal photonic crystals with composition $Si_{1-x}Ti_xO_2$ (x= 0, 0.25, 0.5, 0.75, 1) and photonic band gaps (PBG) spanning the visible spectrum. TiO_2 inverse opals showed *in-vitro* bioactivity for hydroxyapatite growth in simulated body fluids and excellent performance when incorporated in dye sensitized solar cells.

1. Introduction

Photonic crystals are widespread in nature and responsible for the spectacular iridescent colouration shown by many species of bird, butterfly and beetle, as well as the gemstone opal. Photonic crystals are highly ordered materials that possess a periodically modulated refractive index in 1, 2 or 3-dimensions, with periodicity typically on the same length scale as visible light [1]. Such structures can control, manipulate and localize the propagation of light and are characterized by photonic band gaps (PBGs), a narrow range of frequencies for which the propagation of light is forbidden due to coherent Bragg diffraction [2,3]. A colloidal crystal (e.g. opal) is a face-centred cubic (fcc) array of monodisperse colloids with a solid volume fraction of 0.74. Colloidal crystals can be used as templates for the fabrication of inverse opals, materials that comprise a fcc array of air spheres in a solid matrix. The optical properties of opal and inverse opal photonic crystals can be described by a modified Bragg's law which predicts that the PBG position (λ_{max}) is dependent on the interlayer spacing, d, the incident angle of light, θ_{ext}, and average refractive index, n_{avg}, according to

$$\lambda = 2d\sqrt{n_{avg}^2 - \sin^2\theta_{ext}}$$

This work describes the fabrication of inverse opal $Si_{1-x}Ti_xO_2$ (x = 0-1) photonic crystals operating at visible wavelengths using the colloidal crystal template and sol-gel chemistry. Titania inverse opals were evaluated as bio-scaffolds for *in-vitro* hydroxyapatite, $Ca_{10}(PO_4)_6(OH)_2$, formation and as the semiconducting layer in dye-sensitized solar cells (DSSCs).

2. Sample preparation

Monodisperse polymethylmethacrylate (PMMA) colloids with diameters in the range 200-400 nm were synthesized by the surfactant free emulsion polymerization of methyl methacrylate (MMA) at 75 °C [4]. Through careful control of reaction conditions, batches of monodisperse PMMA colloids of different diameter were prepared. PMMA colloidal crystals powders and thin films were fabricated using centrifugation and a flow-controlled vertical deposition, respectively. Sol-gel chemistry was subsequently used to infiltrate the colloidal crystal templates with $Si_{1-x}Ti_xO_2$ (x = 0-1) precursors [4]. Calcination at 450-550 °C removed the PMMA colloidal crystal template and facilitated the thermal decomposition of the sol-gel

precursor leaving behind inverse opal structure which possessed a periodically modulated refractive index with period similar to that of visible light wavelengths.

3. Results

3.1 Characterization of $Si_{1-x}Ti_xO_2$ (x = 0-1) inverse opal photonic crystals

Scanning electron microscopy (SEM) micrographs for a PMMA colloidal crystal template and the resultant $Si_{0.5}Ti_{0.5}O_2$ inverse opal are shown in Fig. 1(a) and (b), respectively. Both the PMMA colloidal crystal template and the inverse opal show a fcc array of spheres with the fcc (111) plane parallel to the underlying glass substrate. The centre-to-centre distance between air spheres (D) on the (111) planes of the inverse opal are slightly less than that between PMMA spheres in the template, indicating a degree of shrinkage during template removal.

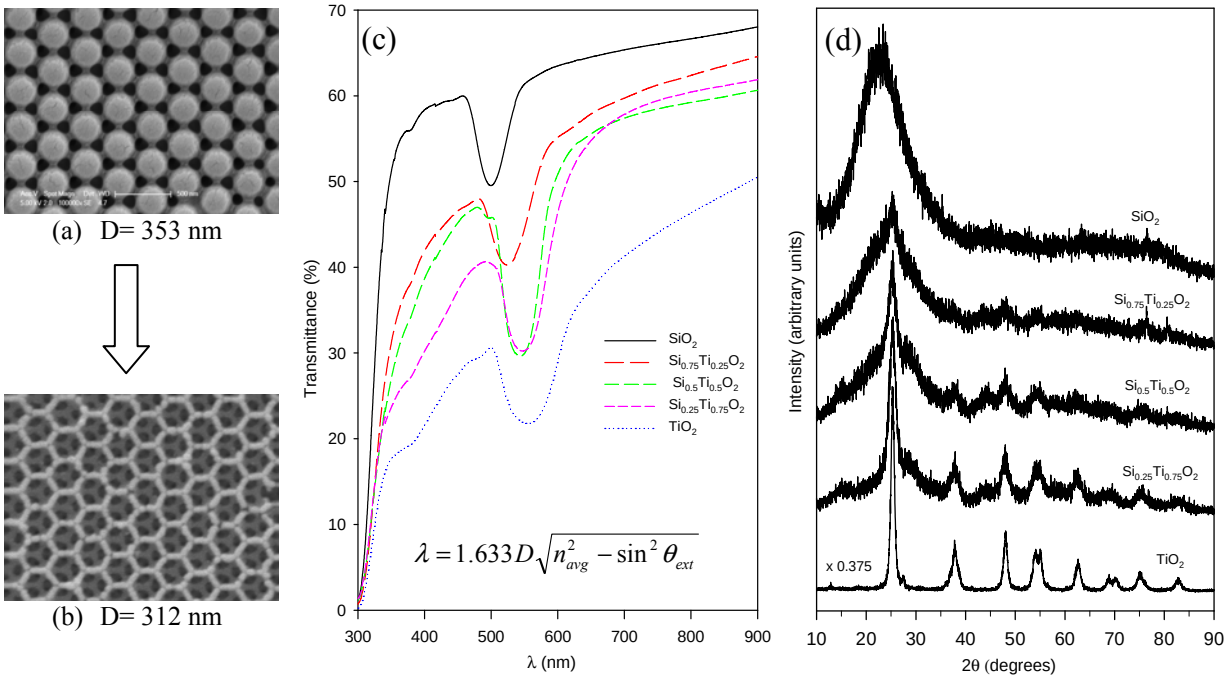

Fig 1. SEM images (left) of (a) PMMA colloidal crystal and (b) corresponding $Si_{1-x}Ti_xO_2$ (x= 0.5) inverse opal; (c) UV-Vis transmittance spectra at normal incidence and (d) XRD patterns for $Si_{1-x}Ti_xO_2$ (x= 0-1) inverse opals.

In UV-Vis transmittance spectra of $Si_{1-x}Ti_xO_2$ (x = 0-1) inverse opals (Fig. 1(c)), intense transmission minima are seen at normal incidence of light (θ = 0°), with respect to the fcc (111) plane. These PBG peaks redshift as the titania molar fraction increases in accordance with the modified Bragg's expression (n_{silica} = 1.45, $n_{titania}$ = 2.1). The width of the PBG peak is related to refractive index of the wall material, and increased on going from SiO_2 to TiO_2. The solid volume fraction also affects the width of the PBG, with a lower solid volume fraction giving a wider PBG. XRD patterns for $Si_{1-x}Ti_xO_2$ (x = 0-1) inverse opals are shown in Fig. 1(d). The silica inverse opal is amorphous. As the TiO_2 content increases, peaks characteristic of nanocrystalline anatase start to appear, whilst the amorphous silica peaks progressively lose intensity.

3.2 Hydroxyapatite formation on TiO_2 inverse opal thin films

SEM images (Fig. 2) show that the surface morphology of the titania inverse opal changed considerably after soaking in a simulated body fluid at ~37 °C for 4 days. This is due to the growth of a thick conformal coating of hydroxyapatite on the inverse opal. Hydroxyapatite is formed due to heterogeneous nucleation by titania [5-7].

The UV-Vis transmittance spectra shown in Fig. 2 (left) indicate that HAP growth shifts the PBG from 555 nm to 664 nm due to the increase in the average refractive index of the photonic crystal after HAP deposition. Powder XRD patterns in Fig. 2 (right) confirm that TiO_2 inverse opal PCs stimulate the growth of HAP as evidenced by the appearance of a new feature at 2θ ~ 32°-33° after SBF treatment. Hence, it can be concluded that *in vitro* assessments using simulated body fluid (SBF) have suggested that inverse opals induce the bonelike apatite formation under physiological conditions [5-7]. Results suggest that titania inverse opals or similar structures could be used as hybrid frameworks for bone regeneration.

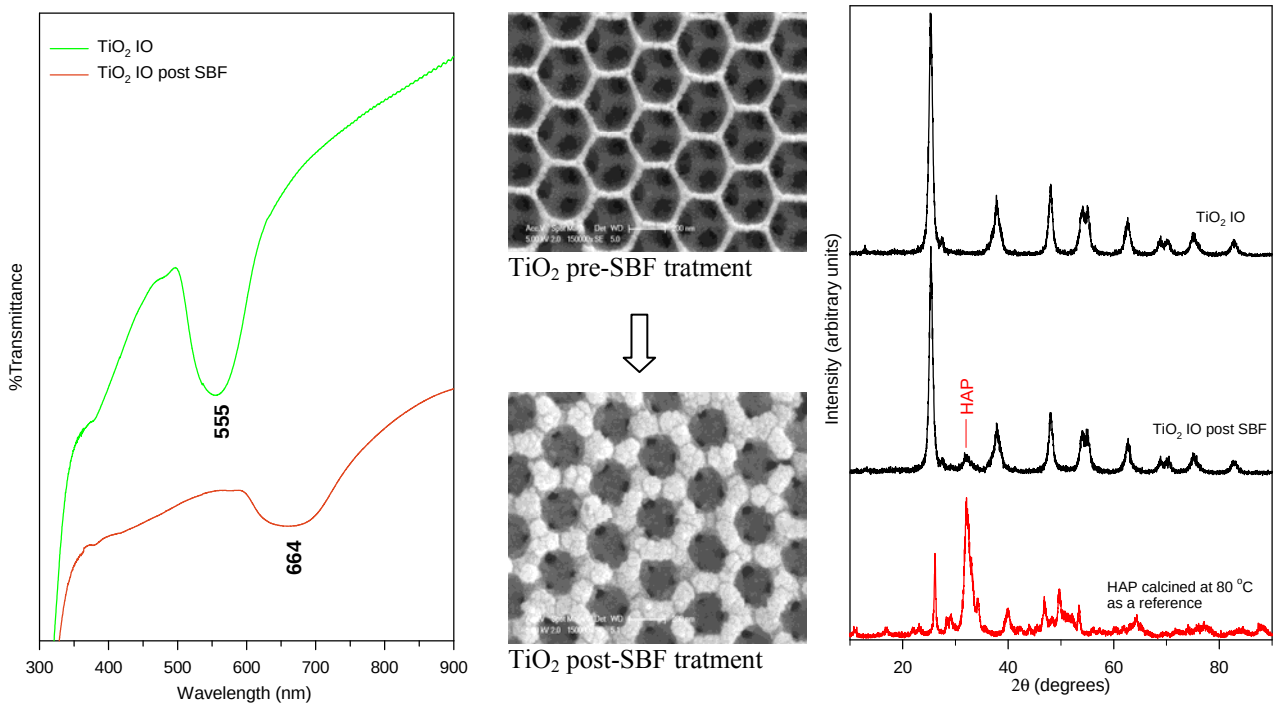

Fig 2. UV-Vis transmittance spectra (left), SEM images (center) and XRD patterns (right) for TiO_2 inverse opal pre- and post- SBF treatment.

3.3 Performance evaluation of DSSCs based on TiO_2 inverse opal thin films

Inverse opal TiO_2 thin films were deposited on indium tin oxide (ITO) conducting glass and used as working electrodes in the assembly of dye sensitized solar cells. A Zn-porphyrin was used as the sensitizer. Fig. 3 illustrates the I-V curves obtained for DSSCs made using three different TiO_2 working electrodes.

Results show that the DSSC constructed using inverse opal TiO_2 thin films gives higher open-circuit voltages, V_{OC}, compared to cells constructed using a reference nanocrystalline titania powder (Table 1). The current density, I_{SC}, and solar conversion efficiency, η (%), of the DSSC increased about twofold on doubling the thickness of TiO_2 inverse opal thin film, although both have similar open-circuit voltages. This indicates that in the bilayer structure, the effective area for dye absorption and light harvesting is doubled. It is noteworthy that the solar conversion efficiencies of cells constructed using the TiO_2 inverse opal bilayer (3.19%) and conventional nanocrystalline TiO_2 (3.65%) are similar, yet the latter cell contains ~10 times more TiO_2. This indicates that the inverse opal structure is able to convert light roughly 10 times more efficiently per gram TiO_2 than the bulk nanocrystalline TiO_2 film. Results confirm that inverse opal titania photonic crystals can be successfully integrated into DSSCs. Higher photon conversion efficiencies could be achieved simply through increasing the TiO_2 inverse opal film thickness.

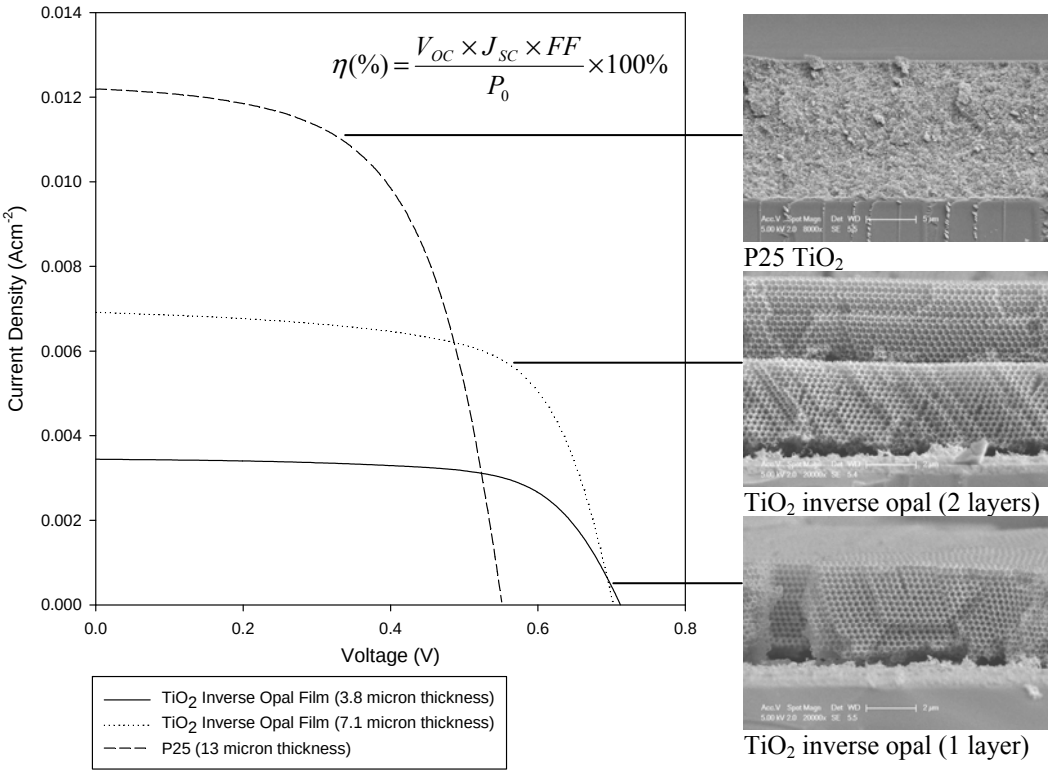

Fig 3. I-V curves for DSSCs (left) prepared using different TiO_2 electrodes (SEM images, right).

Table 1. Summarized results from I-V curves.

Sample	Thickness (μm)	V_{OC} (V)	I_{SC} (mA/cm^2)	FF*	η (%)
TiO_2 inverse opal (1 layer)	3.8	0.712	3.443	0.678	1.62
TiO_2 inverse opal (2 layers)	7.1	0.70	6.915	0.658	3.19
P25 TiO_2 nanocrystalline	13.0	0.584	12.20	0.512	3.65

*FF is the cell fill factor

4. Conclusions

Inverse opal photonic crystals operating at visible wavelengths are easily fabricated by the colloidal crystal template technique. Due to their inherent optical properties, high surface area and macroporous structure, titania inverse are ideal as bio-scaffolds and DSSC electrodes.

References

[1] Moon J H and Yang S 2009 *Chem. Rev.* **110** 547
[2] Nair R and Vijaya R 2009 *Appl. Opt.* **48** 59-63
[3] Yablonovitch E 1993 *J. Opt. Sco. America B.* **10** 283
[4] Waterhouse G I N, Metson J B, Idriss H and Sun-Waterhouse D 2008 Chem. Mat. **20** 1183
[5] Kim H-M, Himeno T, Kokubo T and Nakamura T 2005 *Biomaterials.* **26** 4366
[6] Wang C C and Ying J Y 1999 *Chem. Mat.* **11** 3113
[7] Tang H X, Guo Y P, Jia D C and Zhou Y 2010 *Microporous Mesoporous Mater.* **131** 366